The Orthogonal LMBA: A Novel RFPA Architecture With Broadband Reconfigurability

David J. Collins, *Student Member, IEEE*, Roberto Quaglia, *Member, IEEE*, Jeff R. Powell, Steve C. Cripps, *Life Fellow, IEEE*

***Abstract*—A novel RFPA architecture, the Orthogonal Load Modulated Balanced Amplifier, or OLMBA, is described and demonstrated. Compared to the LMBA, the OLMBA displays many of the same benefits, such as active adaptive tuning using the phase and amplitude of an external control signal, but with much lower power requirements on the control signal power (CSP). As such, a useful range of active tuning can be implemented with essentially no impact on overall efficiency due to the low level of control signal. A demonstrator is described and measured, which delivers 30 W at a minimum of 50% efficiency over a 0.65–3.25 GHz bandwidth.**

***Index Terms*—Power amplifiers, active matching, high efficiency.**

I. Introduction

The ability to change, or optimize, the tuning of an RF Power Amplifier (RFPA) has many potential uses, and can greatly enhance the utility of RFPAs in more conventional applications. Many approaches to implement such tunability have been reported [1], [2], [3]. Such configurations usually show limited tuning range, and suitable low-loss varactors are incompatible with GaAs or GaN RFIC processes. The use of so-called "active" tuning, as an alternative approach to the use of variable reactive elements, has been little used at microwave frequencies. The widely implemented Doherty PA uses load modulation to improve back-off efficiency, but has limited flexibility. More recently, an alternative has emerged, in the so-called "Load Modulated Balanced Amplifier", or LMBA [4], [5], [6], [7]. In this configuration, quadrature couplers are used along with an identical pair of active devices, to form a conventional balanced amplifier. The isolated output coupler port, rather than being terminated, has a "control signal" injection, which is phase coherent, and usually derived from, the input signal. In a seminal paper [4] it was shown that, (a) by varying the magnitude and phase of the injected signal, the load magnitude presented to the balanced devices could be substantially adjusted, with a full phase sweep, and (b) the control signal power (CSP) is entirely recovered at the RF output port. As such, the LMBA has been demonstrated to be a useful alternative to the Doherty, especially in broadband applications [5], [6], [7], [8], [9], [10], [11]. This paper proposes an important evolution of the LMBA; the "Orthogonal LMBA" (OLMBA), whereby the CSP buffer and main PA functions are combined in a single balanced amplifier. The CSP injection is achieved by terminating the output coupler with a reactive element and feeding a much lower level CSP signal into the isolated port of the input coupler. This means that the needed CSP power is much lower compared to the LMBA, relaxing the requirements on its efficient generation. On the other hand, the OLMBA load modulation is not as symmetric as in the LMBA, meaning a more complex behavior which requires extensive non-linear simulations to achieve a successful design.

Manuscript received March 26, 2020; accepted July 17, 2020. Date of publication MM DD, YYYY; date of current version MM DD, YYYY.

D.J. Collins, R. Quaglia and S.C. Cripps are with the Centre for High Frequency Engineering, Cardiff University, Queen's Buildings, The Parade, Cardiff CF24 3AA Wales, UK. e-mail: collinsdj1@cardiff.ac.uk

J.R. Powell is with Skyarna Ltd., Halesowan, West Midlands, U.K. e-mail: jeff.powell@skyarna.com

II. OLMBA Theory

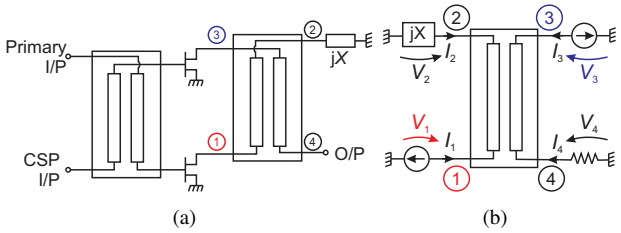

Fig. 1. OLMBA circuit diagram (a) and output section for analysis (b).

Fig. 1(a) shows the schematic diagram of the OLMBA. Rather than injecting the CSP at the output coupler, as it happens in the conventional LMBA, the main signal and the CSP signals are applied to the main and isolated input coupler ports, respectively. Their amplified outputs appear, in principle, separately at the two output coupler ports but the output port which receives the amplified CSP is terminated reactively so that the CSP is reflected back into the balanced stages, thus performing a load modulation function. This configuration has the key advantage compared to the LMBA, that the CSP will always be amplified at the same efficiency as the main signal power, and will be at a much lower level, being scaled down from the signal input, rather than from the output.

The OLMBA configuration for analysis is shown schematically in Fig. 1(b). The output coupler is initially assumed to be a 3 dB quadrature device, with the 4-port Z matrix equations:

$$\begin{cases} jV_1 = \sqrt{2}I_2 + I_3 \\ jV_2 = \sqrt{2}I_1 + I_4 \\ jV_3 = I_1 + \sqrt{2}I_4 \\ jV_4 = I_2 + \sqrt{2}I_3 \end{cases} \quad (1)$$

where the coupler characteristic impedance, Z_0, has been normalized to unity. The CSP input is defined by the parameter

α, which is a voltage scaling factor on the main signal input, and can vary as $0 \leq |\alpha| \leq 1$ in magnitude, but can also be swept over a full range of phase. The output port excitations and terminations add the following relationships:

$$\begin{cases} I_1 = I(-j+\alpha) \\ I_2 = jV_2/X \\ I_3 = I(+1-j\alpha) \\ I_4 = -V_4 \end{cases} \quad (2)$$

Where I is a normalized current magnitude which takes account of the transconductance and input coupler scaling factors; X is normalized to Z_0. Equations (1) can now be solved to determine the balanced device output plane voltages,

$$\begin{cases} V_1 = -j - \alpha\frac{X+j3}{X-j} \\ \\ V_3 = +1 + \alpha\frac{1-j3X}{X-j} \end{cases} \quad (3)$$

Thus the two device voltages both describe a circular trajectory on the complex voltage plane, centered on the unity unmodulated value, as the α CSP parameter varies in magnitude and phase. The corresponding device plane impedances can be determined by dividing the voltages by the respective currents, as given in (3), and are also Smith Chart circles, as shown in Fig. 2(a) for a range of $|\alpha|$ values and for $X = 1$. The Smith Chart is normalized to Z_0. In this specific case, the impedances do not track perfectly as in the LMBA case, but there is still a symmetry in the imaginary part. It must be noted that in the

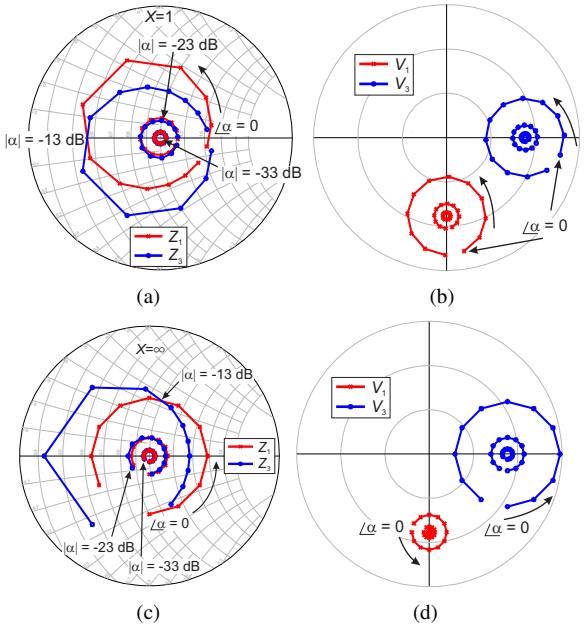

Fig. 2. Impedance (a,c), Voltage (b,d) trajectories in ideal OLMBA at controlled generator planes. $X = 1$ (a,b), $X = \infty$ (c,d). α @ -33,-23,-13 dB. α phase step: 30 degrees.

OLMBA the currents are also imbalanced, so that the device plane voltages can still track quite closely, especially in terms of magnitude. The polar voltage plot is shown in Fig. 2(b); the circle radius is a function of both the magnitude of α and the value of the reactive termination X. When $X = \pm 1$ the radii are equal but the voltages do not precisely track with the phase of α. In practice, this does not detract significantly from the overall utility of the OLMBA. Fig. 2(c) and 2(d) show how the magnitudes of the trajectories can be scaled differentially by adjusting the value of X; this can be used to compensate the asymmetry of a typical coupler response away from the band center. The special cases of jX at open or short circuit with

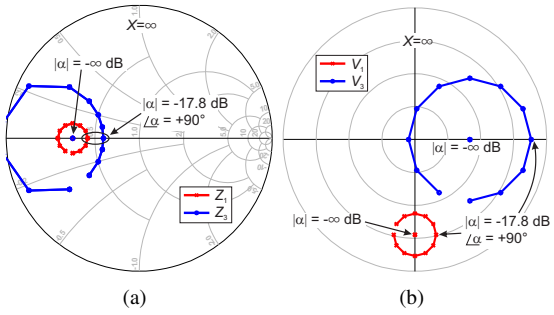

Fig. 3. Impedance and polar voltage with under-coupled coupler ($|S_{41}|$=0.5) in the OLMBA before and after applying the CSP. $X = \infty$ (c,d). α phase step: 30 degrees.

3 dB coupler lead to simplified analysis. On the other hand, Fig. 3 shows the rebalancing concept when an under-coupled coupler ($|S_{41}|$=0.5) is considered. Without CSP action, a much lower voltage magnitude is experienced by one device (V_3), leading to low power and efficiency. On the other hand, by proper choosing α, with $X = \infty$, the voltage magnitude can be equalized and the load impedance kept purely real, hence recovering efficiency and a good portion of the output power.

III. Demonstrator Design

The demonstration design described in this section was intended primarily as a verification that active tuning can perform a useful function with very low expenditure of control signal power. Most notably, the active tuning can replace complex multi-section passive matching networks and offer flexibility for post-manufacture tuning. A photograph of the

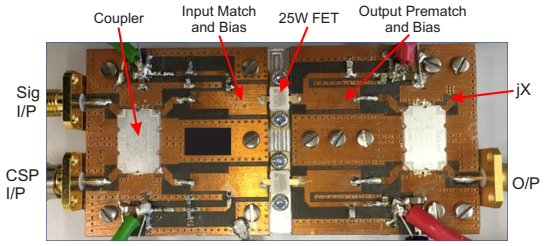

Fig. 4. Demonstrator board picture. (Size: 86 mm × 42 mm).

demonstrator board is shown in Fig. 4. Input and output couplers were the Anaren 11306-3S which operates between 2 and 4 GHz. Note that this coupler would not normally be considered suitable for implementing a balanced PA to cover the design bandwidth of the demonstrator, especially in the lower end of the band. On the other hand, this is useful to demonstrate that, as suggested in Fig. 5, the OLMBA action can be used to recover part of the performance where the coupler is unbalanced. The transistors were the 25 W Wolfspeed CGH40025F. This device has an optimum power match

in the region of 10-15 Ω; instead on relying on a complex matching network, the idea has been instead to exploit the OLMBA action and a single section of pre-matching only has been used. The pre-matching has been adjusted, using large

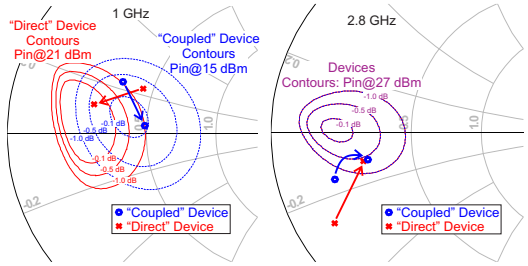

Fig. 5. Simulated loads, moving from "no CSP" to "with CSP" condition.

simulations where α and X were swept, so that OLMBA action could bring the synthesized loads within the optimum load regions of the device. Fig. 5 shows this concept at two frequencies. At 2.8 GHz, the coupler is in-band and the load modulation is used to move the loads using as reference the same power contours at saturation. On the other hand, at 1 GHz the coupler is heavily undercoupled, so the reference contours for the coupled device are at lower input power (≃-6 dB) with respect to the other device (evaluated at saturation).

The reactive termination X was implemented on this test circuit as replaceable SMT components. Fig. 6 shows a simulation of the power output and PAE showing the effect of using CSP with $|\alpha|$ @ -10 dB, and varying X and phase of α. Note that at each frequency the performance can be maximized with proper X and α, as highlighted by the enveloping red line. The drain/gate voltage were at 28 V/-2.85 V, respectively, with quiescent drain current of 30 mA/device.

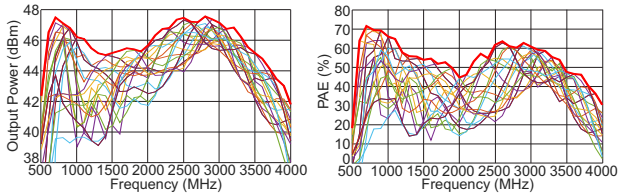

Fig. 6. Simulated Output power and PAE vs. frequency, with $|\alpha|$ @ -10 dB. With varying X and phase of α.

For the purposes of demonstration and evaluation, the demonstration board was tested using two separate inputs using phase locked CW generators. This enabled full phase sweeps to be performed on the CSP signal input under bus control. Also, the X value was varied by changing the termination manually and testing different cases (open circuit, 100 pF capacitor, 1.6 pF capacitor, 5 nH inductor). No large signal instability was observed, however, the fact of using circulators on the input ports might have helped since the OLMBA potentially unbalances a balanced structure with a serious risk for odd-mode oscillations to appear. Where circulators cannot be used, attention should be paid to this aspect. Fig. 7 shows the PAE vs. output power obtained from power sweeps at different frequencies, in the open circuit condition for X. The black squares show the case without CSP

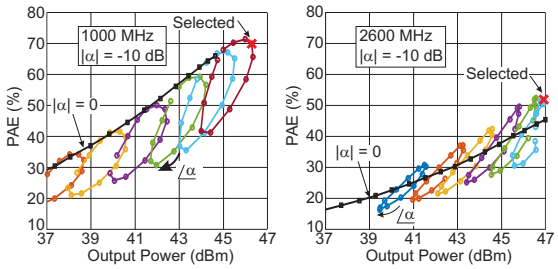

Fig. 7. Measured PAE vs. Output power, with X at open circuit. With no CSP (black squares) and with $|\alpha|$ @ -10 dB, with 30 degree phase steps (colored circles), at different input power levels.

(jX at open circuit), the colored traces with circles indicate the result of sweeping the phase with CSP power at constant -10 dB from the main input. The effect of OLMBA action is quite different at the two frequencies selected as examples. At 1 GHz, the CSP allows increasing the output power of around 1.5 dB, while the PAE was already very good without OLMBA action and is only slightly increased. On the other hand, at 2.6 GHz, the output power was already around 50 W without CSP, but applying OLMBA action the PAE was increased from 45% to 52% without loss of output power. The results of similar sweeps are analyzed from 600 MHz to 3300 MHz, and the best combination of X and phase setting (as indicated in Fig. 7) is selected to build-up the plots in Fig. 8. These show the output power, PAE and gain vs. frequency,

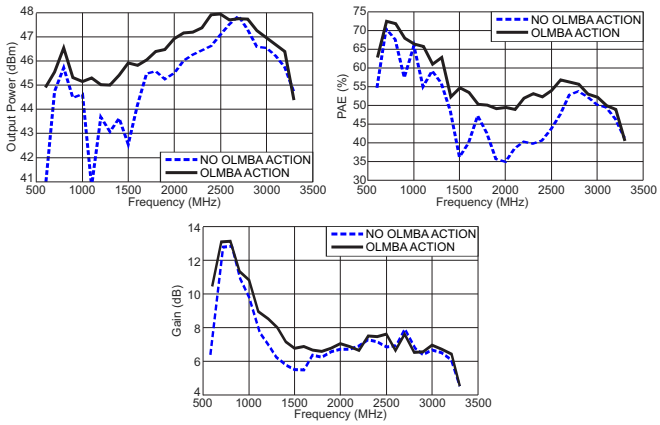

Fig. 8. Measured output power, PAE, and gain with and without OLMBA action, vs. frequency.

comparing the performance with and without OLMBA action. The aim of this comparison is demonstrating that the CSP action is present and effective, not that this OLMBA is better than an optimised PA working on this band. The OLMBA action allows pushing the output power above 45 dBm, and the PAE above 50%, across a 650-3250 MHz band.

IV. Conclusion

The OLMBA offers a versatile option for active matching in high frequency amplifiers, providing an effective way of amplifying the CSP signal without additional amplifiers aiming to maximise overall circuit efficiency. A striking aspect is how the performance can be maintained over a 4:1 bandwidth using a coupler which is not optimized for this bandwidth.

REFERENCES

[1] H. M. Nemati, et al., "Design of varactor-based tunable matching networks for dynamic load modulation of high power amplifiers," *IEEE Trans. on Microw. Theory and Techn.,* vol. 57, pp. 1110–1118, May 2009.

[2] C. Sanchez-Perez, et al., "Optimized design of a dual-band power amplifier with SiC varactor-based dynamic load modulation," *IEEE Trans. on Microw. Theory and Techn.,* vol. 63, pp. 2579–2588, Aug 2015.

[3] S. Zha, et al., "Design of adaptive highly efficient GaN power amplifier for octave-bandwidth application and dynamic load modulation," *IEEE Trans. on Microw. Theory and Techn.,* vol. 60, pp. 1829–1839, June 2012.

[4] D. J. Shepphard, et al., "An efficient broadband reconfigurable power amplifier using active load modulation," *IEEE Microwave and Wireless Components Letters,* vol. 26, pp. 443–445, June 2016.

[5] R. Quaglia, S.C. Cripps, "A Load Modulated Balanced Amplifier for Telecom Applications", *IEEE Trans. on Microw. Theory and Techn.,* vol. 66, pp.1328–1338, Mar 2018.

[6] P. H. Pednekar, et al., "RF-input load modulated balanced amplifier with octave bandwidth," *IEEE Trans. on Microw. Theory and Techn.*, vol. 65, pp. 5181–5191, Dec 2017.

[7] D. Collins, et al., "Experimental characterization of a load modulated balanced amplifier with simplified input power splitter" in 2018 Asia-Pacific Microwave Conference (APMC), pp. 461–463, Nov 2018.

[8] P. H. Pednekar, et al., "Analysis and Design of a Doherty-Like RF-Input Load Modulated Balanced Amplifier," *IEEE Trans. on Microw. Theory and Techn.*, vol. 66, no. 12, pp. 5322-5335, Dec. 2018.

[9] T. Cappello, et al., "Supply- and Load-Modulated Balanced Amplifier for Efficient Broadband 5G Base Stations," *IEEE Trans. on Microw. Theory and Techn.*, vol. 67, no. 7, pp. 3122-3133, July 2019.

[10] Y. Cao, et al., "Load Modulated Balanced Amplifier with Reconfigurable Phase Control for Extended Dynamic Range," in 2019 IEEE MTT-S Intern. Microw. Symp., pp. 1335-1338, June 2019.

[11] J. Pang, et al., "Analysis and Design of Highly Efficient Wideband RF-Input Sequential Load Modulated Balanced Power Amplifier," *IEEE Trans. on Microw. Theory and Techn.*, vol. 68, no. 5, pp. 1741-1753, May 2020.